Supporting Information

Direct Imprinting of Thermally Reduced Silver Nanoparticles *via* Deformation-Driven Ink Injection for High-Performance, Flexible Metal Grid Embedded Transparent Conductors

Y. S. Oh,[a] D. Y. Choi[a] and H. J. Sung[a]*
[a]Department of Mechanical Engineering, KAIST
291 Daehak-ro, Yuseong-gu, Daejeon 34141, Korea
*E-mail: hjsung@kaist.ac.kr

Keywords: direct imprinting, mold deformation, embedding, metal grid, transparent conductors.

Fig. S1(a) show a cross-sectional schematic illustration of the Ag ion ink captured inside the cavity of the deformed mold at low and high pressures during the solvent evaporation and the thermal reduction of Ag ions. The behavior which Ag ion ink was captured inside the deformed mold at different pressures could be explained by considering Poiseuille's law, [1]

$$q = \frac{\Delta P h_f^{\,4}}{12 \mu L_f}, \qquad (2)$$

where ΔP is the pressure difference inside and outside of the mold cavity, q is the ink flow out of the mold cavity, h_f is the film thickness between the mold and the substrate, μ is the dynamic viscosity of the Ag ion ink, and L_f is the distance between the mold cavity and the outside edge of the mold. The mold is floated on a liquid film where h_f is inversely proportional to ΔP. At low pressures, most of the ink left from the mold cavity due to the large value of h_f. As the meniscus of the liquid rapidly ruptured in the center of the mold cavity, small amounts of the Ag NPs are deposited near the bottom edges of the deformed walls on the substrate. On the other hand, the Ag ion ink is captured inside the deformed cavity due to the small value of h_f at high pressures. As the meniscus of the liquid slowly slips down the side walls of the deformed mold, the Ag NP structures are fabricated within the deformed cavity.

Fig. S1(b) shows microscope images of the metal grid structures fabricated under three different pressure conditions. At P = 35 kPa, small amounts of Ag NPs were deposited between the bottom edges of the deformed walls and the substrate. Most of the Ag ion ink leaked out of the mold cavity during the reduction of Ag ions. The Ag NP structures were not connected, but were isolated from the neighboring structures. At P = 70 kPa, these structures were successfully fabricated, and connected with all of the structures due to the capture of ink. At higher pressures of P = 140 kPa, excessive deformations of the mold cavity reduced the

amount of ink present inside the considerably reduced volume. The Ag NP structures that yielded a wide thin film (8 μm) with a low height profile (< 500 nm), were smaller than the dimensions of structures fabricated at P = 70 kPa.

Fig. S1(c) shows the sheet resistances and transmittance spectra obtained from the metal grid TCs, fabricated using R-mold at different temperatures ranging from 50 °C to 80 °C. All of them showed superior performance of R_s (< 10 Ω/sq) and T at 550 nm (> 90 %). However, the spectral intensity did decrease for T (350-500 nm) at T_o = 70-80 °C. A sharp decrease was observed at T_o = 80°C. These feature were attributed to the excitation of the local surface plasmon resonance (LSPR) in the residual layers. [2]

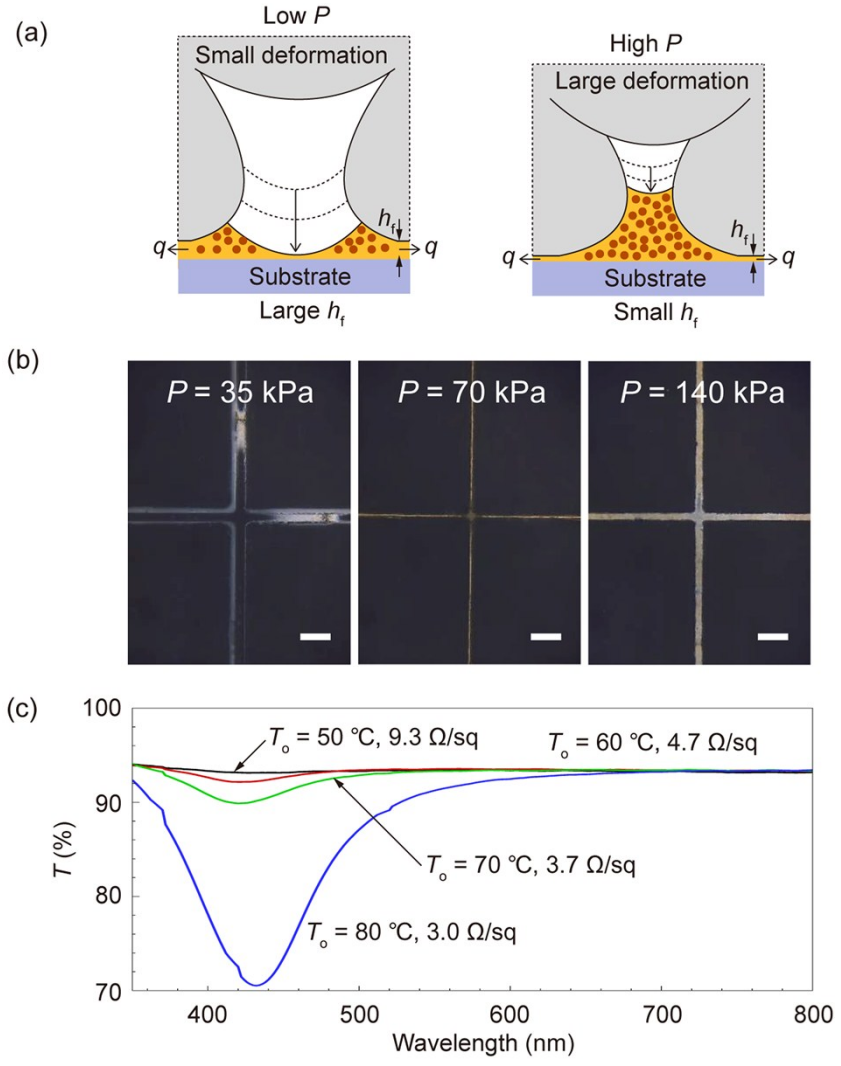

Fig. S1 (a) Cross-sectional schematic illustration of the unconfined Ag ion ink or the ink confined inside the mold cavity at a low P or a high P, respectively. (b) Optical microscopy images in the metal grid under different pressures (scale bar: 20 μm). (c) Sheet resistances and transmittances spectra of the metal grid TCs fabricated at different T_o values.

1. W. Cheng, N. Park, M. T. Walter, M. R. Hartman and D. Luo, *Nat. Nanotechnol.*, 2008, **3**, 682-690.
2. J. Groep, P. Spinelli and A. Polman, *Nano Lett.*, 2012, **12**, 3138-3144.

Fig. S2(a) and (b) show AFM images of line structures fabricated at AR = 0.5 and 1, respectively. The line structures were locally destroyed or were much smaller than the line structures formed using the R-mold. Fig. S2(c) The R_s and T at 550 nm of the metal grid TCs fabricated using the T-mold at the three different AR values of 0.5, 0.75, and 1. The best performance of the metal grids fabricated using the T-mold was achieved at AR = 0.75.

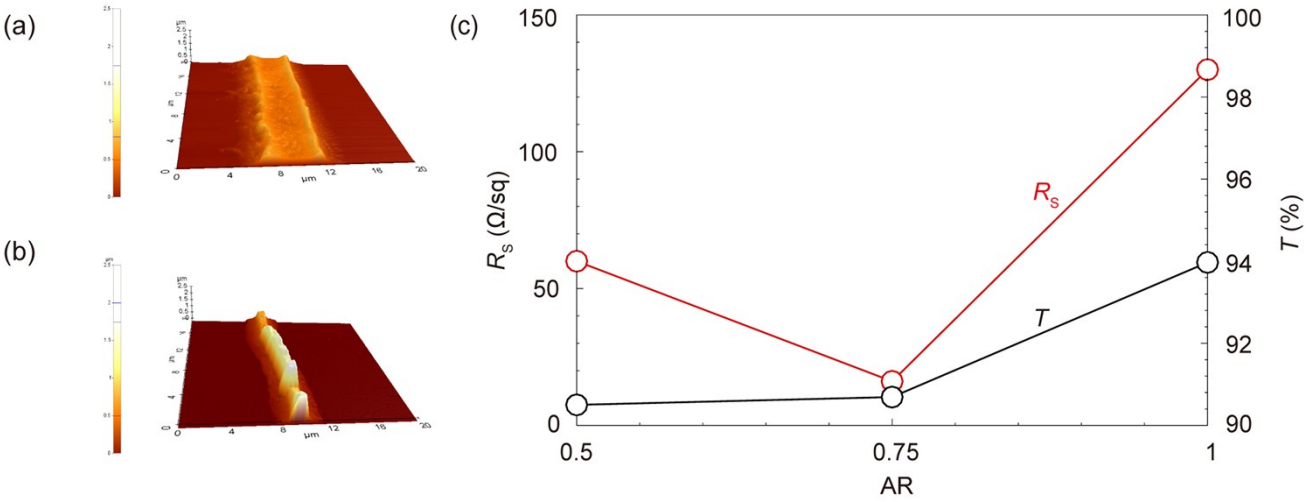

Fig. S2 AFM images of the metal grid line fabricated using the T-mold at (a) AR = 0.5 and (b) AR = 1, respectively. (c) The R_s and T at 550 nm of the metal grid TCs fabricated using T-mold at different ARs.

Fig. S3 shows AFM surface profiles of the embedded metal grid and NOA 81 in which a groove was generated by the wettability of NOA 81. As a re-fluorinated treatment time decreased from 3 min to 10 sec, the groove depth was only reduced from 1 μm to 500 nm with keeping its width (~ 2 μm). The heating process after the re-fluorinated treatment for 1 min resulted in the reduction of the groove depth and width from ~ 1 μm and ~ 2 μm to ~ 200 nm and ~ 1 μm, respectively.

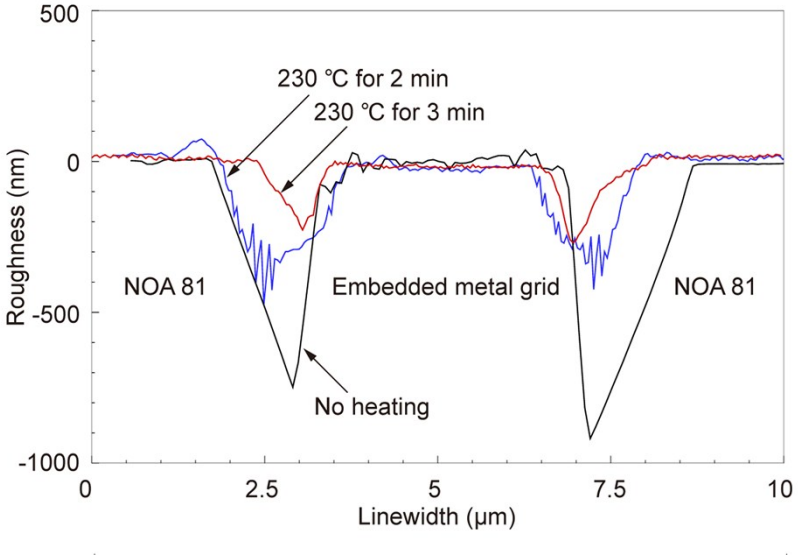

Fig. S3 AFM surface profiles of the embedded metal grid and the NOA 81 by the heating process after the fluorinated treatment.